HHS Public Access

Author manuscript

Nat Immunol. Author manuscript; available in PMC 2013 May 01.

Published in final edited form as:

Nat Immunol. 2012 November ; 13(11): 1101–1109. doi:10.1038/ni.2423.

TBK1 controls IgA class switching by negatively regulating noncanonical NF-κB signaling

Jin Jin[1], **Yichuan Xiao**[1], **Jae-Hoon Chang**[1], **Jiayi Yu**[1], **Hongbo Hu**[1], **Robyn Starr**[3], **George C. Brittain**[1], **Mikyoung Chang**[1], **Xuhong Cheng**[1], and **Shao-Cong Sun**[1,2]

[1]Department of Immunology, The University of Texas MD Anderson Cancer Center, 7455 Fannin Street, Box 902, Houston TX 77030, USA

[2]The University of Texas Graduate School of Biomedical Sciences at Houston, Houston, Texas 77030, USA

[3]St. Vincent's Institute, 41 Victoria Parade, Fitzroy, Victoria 3065, Australia

Abstract

Immunoglobulin (Ig) class switching is crucial for generating antibody diversity in humoral immunity and, if deregulated, also has severe pathological consequences. How the magnitude of Ig isotype switching is controlled is still poorly understood. Here we identify TANK-binding kinase 1 (TBK1) as a pivotal negative regulator of IgA class switching. B cell-specific TBK1 ablation in mice resulted in uncontrolled production of IgA and development of nephropathy-like disease symptoms. TBK1 negatively regulated IgA class switching by attenuating noncanonical NF-κB signaling, an action that involved TBK1-mediated phosphorylation and subsequent degradation of the NF-κB-inducing kinase. These findings establish TBK1 as a pivotal negative regulator of the noncanonical NF-κB pathway and highlight a unique mechanism that controls IgA production.

Keywords

IgA; Ig class switching; TBK1; NF-κB; noncanonical NF-κB

INTRODUCTION

B cells serve as the primary player of humoral immune responses against infections but are also responsible for various autoimmune disorders. Upon activation by an antigen, mature B cells proliferate and undergo a series of differentiation events, including immunoglobulin

Correspondence should be addressed to S.-C. S. (ssun@mdanderson.org).

AUTHOR CONTRIBUTIONS

J.J. designed and did the research, prepared the figures, and wrote part of the manuscript; Y.X., J.-H.C., J.Y., H.H., G.C.B., M.C., and X.C. contributed experiments; R.S. contributed reagents; and S.-C.S. designed the research and wrote the manuscript.

COMPETING FINANCIAL INTERESTS

The authors declare no competing financial interests.

(Ig) class switching to acquire the ability to produce various antibody isotypes with specialized effector functions. In particular, IgA has an important role in mediating mucosal immunity, and its deficiency is a commonly seen primary immunodeficiency in humans[1-3]. Conversely, IgA production is tightly controlled, since its deregulation contributes to the pathogenesis of severe diseases, such as IgA nephropathy, characterized by elevated serum IgA concentrations and antibody deposition within kidney glomeruli as well as symptoms of kidney dysfunction[4-6]. Induction of IgA class switching involves different signals, most importantly by stimulation via transforming growth factor-β (TGF-β) and costimulatory signals triggered by CD40 ligand (CD40L) or its related tumor necrosis factor (TNF) family members, BAFF and APRIL[7-12].

A common signaling function of the TNF receptor (TNFR) family members is activation of NF-κB, a family of transcription factors with diverse functions in the immune system[13, 14]. Activation of NF-κB is mediated by canonical and noncanonical pathways[13-15]. While the canonical pathway has been extensively studied, much remains to be investigated regarding the regulation and functions of the noncanonical pathway. This latter pathway depends on NF-κB inducing kinase (NIK) and its downstream kinase IKKα, which induces the processing of p100, an NF-κB precursor protein that also functions as a cytoplasmic inhibitor of NF-κB. The processing of p100 not only generates a mature NF-κB subunit, p52, but also leads to nuclear translocation of the sequestered NF-κB members[15]. Although p52-RelB is the major NF-κB complex induced by the noncanonical NF-κB pathway, it may also contribute to the activation of other NF-κB members in B cells[16]. Consistently, mice expressing an inactive NIK mutant or a processing-deficient p100 mutant (Lym1) have much more severe immune defects than the p52- and RelB-deficient mice[16-20].

Unlike the canonical NF-κB pathway, which responds to diverse stimuli, the noncanonical NF-κB pathway selectively responds to a small subset of TNFR family members, including CD40 and BAFF receptor (BAFFR) whose ligands are CD40L and BAFF, respectively[21]. A related TNFR member, TACI (transmembrane activator and calcium-modulating cyclophilin ligand interactor), recognizes both BAFF and APRIL and also induces the noncanonical NF-κB pathway, albeit less so[21-24]. Although the role of noncanonical NF-κB pathway in IgA class switching has not been definitively demonstrated, accumulating evidence suggests this possibility. Mice carrying a *Map3k14* mutation, or mice expressing the processing-defective Lym1 p100 mutant, have severe defects in IgA production[16, 17]. Bone marrow adoptive transfer studies further indicate a function of NIK in hematopoietic cells that regulates the systemic production of IgA[25]. Moreover, overexpression of the noncanonical NF-κB inducer BAFF in B cells causes IgA hyperproduction and IgA nephropathy[5, 6]. However, despite these functional connections, how the signal-induced noncanonical NF-κB activation and IgA class switching are controlled remains unknown.

TANK-binding kinase 1 (TBK1), as well as its homologue, IKKε (also called IKKi), are known as innate immune regulators that mediate induction of type I interferons (IFNs) in response to Toll-like receptor (TLR) stimulation and viral infection[26-30]. However, due to the embryonic lethality of the TBK1 conventional knockout (KO) mice[31], the *in vivo* biological functions of TBK1 has remained largely unknown. In the present study, we generated B cell-conditional *Tbk1* mice (hereafter called *Tbk1*^{BKO} mice). Our studies led to

the discovery of an unexpected and quite remarkable function for TBK1 in the control of IgA class switching. TBK1 inhibits IgA class switching by specifically opposing the signaling function of the TNF family members, and this in turn involves the attenuation of noncanonical NF-κB activation. TBK1 mediates phosphorylation and degradation of NIK, thereby preventing aberrant accumulation of this central signaling component of the noncanonical NF-κB pathway. These findings establish TBK1 as a critical regulator of IgA class switching, suggesting a pivotal role for TBK1 in controlling noncanonical NF-κB signaling.

RESULTS

TBK1^{BKO} mice aberrantly produce IgA and autoantibodies

To study the *in vivo* function of TBK1 in regulating humoral immune responses, we crossed *Tbk1*-floxed mice with CD19-Cre mice to generate *Tbk1*$^{fl/fl}$*Cd19*^{Cre} (hereafter called *Tbk1*^{BKO}) and *Tbk1*$^{+/+}$*Cd19*^{Cre} wild-type control mice (Supplementary Fig. 1). Unlike conventional *Tbk1*$^{-/-}$ mice, the *Tbk1*^{BKO} mice were born with expected Mendelian ratio and grossly normal in growth and survival. The B cell-specific TBK1 ablation also did not affect B cell development and maturation, as suggested by the presence of comparable B cell subpopulations in the spleen (Supplementary Fig. 2) and bone marrow (**data not shown**) of the *Tbk1*^{BKO} and wild-type mice.

To examine the *in vivo* role of TBK1 in B cell activation and differentiation, we immunized the wild-type and *Tbk1*^{BKO} mice with 4-hydroxy-3-nitrophenyl acetyl (NP)-keyhole lympet hemocyanin (KLH), NP-lipopolysaccharide (LPS), and NP-Ficoll, representing TD, TI-1, and TI-2 antigens, respectively. The production of antigen-specific IgM was moderately enhanced in the mutant animals, whereas the production antigen-specific IgG was not significantly altered (Fig. 1a). The production of individual IgG isotypes was either not significantly affected or moderately reduced in the *Tbk1*^{BKO} mice (Fig. 1b). Remarkably, the *Tbk1*^{BKO} mice produced a substantially more antigen-specific IgA compared to the wild-type mice (Fig. 1a).

Under unimmunized conditions, the *Tbk1*^{BKO} and age-matched wild-type control mice had comparable concentrations of serum IgM and IgG throughout of the ages analyzed (Fig. 1c). At young ages (3-9 weeks), the *Tbk1*^{BKO} mice also did not show obvious abnormalities in their steady-state abundance of serum IgA; however, starting from 12 weeks of age, these mutant animals had significantly increased serum IgA concentrations when compared to age-matched wild-type control mice (Fig. 1c). The older *Tbk1*^{BKO} mice (8 month) also had increased serum titers of anti-nuclear antigen (ANA) and anti-double-stranded DNA (dsDNA) autoantibodies (Fig. 1d) as well as prominent antibody deposition in the kidney glomeruli (Fig. 1e), a major pathological feature of nephropathy[32]. These older mutant animals also displayed additional nephropathy symptoms, including increased concentrations of urinary protein, serum nitrogen and creatinine (Fig. 1f). Thus, TBK1 expression in B cells is critical for maintaining normal production of IgA and preventing nephropathy-like disorders.

TBK1 inhibits CD40- and BAFF-induced IgA class switching

The aberrant production of IgA by the *Tbk1*^{BKO} mice prompted us to examine the role of TBK1 in regulating IgA class switching. Consistent with their elevated concentrations of serum IgA, older *Tbk1*^{BKO} mice contained a markedly higher frequency of IgA^{+} B cells in mesenteric lymph nodes (MLNs) and Peyer's patches (PPs) (Fig. 2a), lymphoid organs known to be active in IgA class switching[12]. Upon immunization with a TD antigen, the young *Tbk1*^{BKO} mice also displayed a significantly increased frequency and number of IgA^{+} B cells in the spleen (Fig. 2b). In contrast, the frequency of IgM^{+} and IgG1^{+} B cells was either not influenced or even reduced in the *Tbk1*^{BKO} mice. B-cell adoptive transfer studies revealed that the *Tbk1*^{BKO} B cells produced significantly more IgA^{+} B cells than wild-type B cells in both single transfer and mixed transfer experiments (Supplementary Fig. 3). These findings emphasize a B cell-intrinsic role for TBK1 in regulating IgA^{+} B cell production.

We further examined the role of TBK1 in regulating IgA class switching using a well-characterized *in vitro* protocol based on the induction of IgA class switching by TGF-β and the TNF family members, CD40L, BAFF and APRIL[11]. Interestingly, the *Tbk1* deficiency did not significantly alter the TGF-β-stimulated IgA switching but greatly promoted the induction of IgA^{+} B cells (Fig. 2c,d) and secreted IgA (Fig. 2d, bottom) by anti-CD40 and BAFF. Similar results were obtained when the IgA class-switching was performed by using an agonistic IgM antibody, instead of LPS, as B cell activator (data not shown). To compare the role of TBK1 in regulating the class switching to IgA and other Ig isotypes, we employed a modified protocol involving the replacement of TGF-β and APRIL with IL-4, which is known to stimulate class switching to both IgA and other isotypes such as IgG1[9, 33]. As seen under the TGF-β class-switching condition, the TBK1 deficiency caused aberrant induction of IgA^{+} B cells by anti-CD40 and BAFF (Supplementary Fig. 4a,b). Although the TBK1 deficiency also promoted BAFF-induced IgG1 production, this effect was much weaker (Supplementary Fig. 4a,b). Thus, TBK1 has a predominant role in controlling IgA class switching.

Immunoglobulin class switching is initiated by the expression of germline transcripts (GLT) and requires activation-induced cytidine deaminase (*Aicda*)[34, 35]. We found that the TBK1 deficiency promoted the induction of both the alpha GLT (αGLT*)* and *Aicda* by anti-CD40 and BAFF, although the effect on αGLT induction was predominantly seen with BAFF stimulation (Fig. 2e). This effect of BAFF was not limited to the TGF-β class-switching condition, since similar results were obtained with the IL-4 class-switching condition (Supplementary Fig. 4c). In contrast, the TBK1 deficiency did not significantly enhance the induction of the gamma 1 GLT (γ1GLT) (Supplementary Fig. 4c). Collectively, these results suggest a critical role for TBK1 in negatively regulating IgA class switching, thus explaining the aberrant IgA production in *Tbk1*^{BKO} mice.

TBK1 regulates IgA production independently of type I IFN

TBK1 and IKKε are structurally related kinases that mediate type I IFN induction in antiviral innate immunity[36, 37]. We found that LPS-stimulated IRF3 phosphorylation and type I IFN expression was inhibited in the *Tbk1*^{BKO} B cells (Fig. 3a,b). However, the IgA-regulating function of TBK1 was independent of the autocrine action of type I IFNs, since

ablation of the type I IFN receptor (IFNAR) in *Tbk1*^{BKO} mice failed to correct the IgA hyper-production phenotype (Fig. 3c). Consistently, B cells derived from the *Tbk1*^{BKO}*Ifnar*^{KO} mice remained to be hyper-sensitive to anti-CD40 and BAFF in the production of IgA^{+} B cells (Fig. 3d) and the expression of αGLT and *Aicda* (Fig. 3e). We also found that in sharp contrast to the TBK1-deficient B cells, the IKKε-deficient B cells did not display any obvious abnormalities in IgA class switching (Fig. 3f). Thus, the TBK1-mediated control of IgA class switching is independent of type I IFN signaling and not seen with its homologue IKKε.

TBK1 negatively regulates noncanonical NF-κB signaling

A major signaling function of the TNF family of IgA-costimulators is NF-κB activation. Unlike LPS and anti-BCR, which only induce the canonical NF-κB pathway, BAFF and anti-CD40 are potent inducers of the noncanonical NF-κB pathway[15]. In addition, although the major target of APRIL is the canonical NF-κB pathway, APRIL also weakly stimulates the noncanonical NF-κB pathway[21-23, 38, 39]. In response to the canonical NF-κB inducers, LPS or anti-IgM, the TBK1-deficient B cells had a moderate increase in NF-κB activation (Fig. 4a and data not shown). The APRIL-induced NF-κB was comparable between the wild-type and *Tbk1*^{BKO} B cells during the early phase of stimulation, although it was enhanced in the TBK1-deficient B cells during the late-phase of stimulation (Fig. 4b). Remarkably, the *Tbk1* deficiency greatly enhanced the activation of NF-κB induced by anti-CD40 and BAFF (Fig. 4c,d). These findings were in agreement with the major effect of *Tbk1* deficiency on IgA induction by anti-CD40 and BAFF.

In vitro kinase assays revealed that loss of TBK1 only weakly promoted the activation of IKK by LPS and did not affect the anti-CD40-stimulated IKK activation (Supplementary Fig. 5a). Since anti-CD40 and BAFF stimulate the noncanonical NF-κB pathway[15], we reasoned that TBK1 might have a major role in regulating this specific NF-κB pathway. Indeed, the anti-CD40- and BAFF-stimulated activation of nuclear p52 and RelB was greatly enhanced in the TBK1-deficient B cells as compared to wild-type B cells (Fig. 4e,f). This result was associated with a greater loss of the p52 precursor protein p100 in the cytoplasm of the mutant B cells (Fig. 4e,f), thus suggesting a role for TBK1 in negatively regulating the induction of p100 processing. This function of TBK1 was not due to an alteration of the surface receptor expression, since the *Tbk1*^{BKO} and wild-type B cells expressed comparable amounts of CD40, BAFFR, and TACI (data not shown). Furthermore, the *Tbk1* deficiency did not promote the activation of p50 or c-Rel and only moderately enhanced the activation of RelA (Supplementary Fig. 5b). The moderate enhancement in RelA activation in the *Tbk1*^{BKO} cells was consistent with the contribution of p100 processing to RelA activation[16]. Taken together, these results established TBK1 as a pivotal negative regulator of the noncanonical NF-κB signaling pathway.

Noncanonical NF-κB pathway regulates IgA class switching

Prior studies suggested a role for the noncanonical NF-κB pathway in regulating IgA production[6, 16, 17, 25], although direct evidence for its involvement in IgA class switching has been lacking. To address this question, we took the advantage of the NIK-deficient mice, which are defective in noncanonical NF-κB signaling[15, 40]. The NIK-deficient B cells were

largely normal in TGF-β-induced IgA class switching; however, they were defective in the induction of IgA class switching by anti-CD40 and BAFF, as assessed by the frequency of IgA^+ B cells (Fig. 5a,b). We also employed mutant mice harboring an *Nfkb2* gene mutation (called Lym1), which results in the production of a nonprocessible form of p100 and, thus, the blockade of noncanonical NF-κB activation[16]. Both homozygous *Nfkb2*$^{lym1/lym1}$ and heterozygous *Nfkb2*$^{lym1/+}$ mice have severe immune deficiencies, including attenuated IgA production[16]. We found that in response to anti-CD40 or BAFF, the *Nfkb2*$^{lym1/+}$ B cells displayed a severe defect in the production of IgA^+ B cells (Fig. 5c). Using the IL-4-based class-switching condition, we demonstrated that the NIK deficiency and *Nfkb2*^{Lym1} mutation only weakly reduced anti-CD40- and BAFF-mediated induction of $IgG1^+$ B cells, while these genetic changes severely inhibited the induction of IgA^+ B cells (Supplementary Fig. 6a). Consistently, the NIK deficiency and *Nfkb2*^{lym1} mutation severely attenuated anti-CD40- and BAFF-induced expression of αGLT but only had a weak or no effect on the induction of γ1GLT (Supplementary Fig. 6a). These results further suggest that the noncanonical NF-κB has a predominant role in promoting IgA class switching, although it may also be involved in the induction of other antibody isotypes.

We next examined the involvement of noncanonical NF-κB in mediating the IgA hyper-production in TBK1-deficient B cells by crossing *Tbk1*^{BKO} mice with NIK-deficient mice. While TBK1 deficiency in NIK-competent mice caused a substantial increase in antigen-induced production of IgA^+ B cells, loss of TBK1 in the NIK-deficient background did not appreciably promote the production of IgA^+ B cells (Fig. 5d and Supplementary Fig. 6b). Furthermore, the B cell ablation of TBK1 in the NIK-deficient background also did not cause the abnormal increase in antigen-specific serum IgA (Supplementary Fig. 6c). Thus, the noncanonical NF-κB pathway appears to be responsible for the IgA hyper-production in the *Tbk1*^{BKO} mice.

To rule out the possible involvement of B cell development in the IgA class-switching defect of the NIK-deficient B cells, we performed shRNA-mediated NIK knockdown in wild-type and *Tbk1*^{BKO} B cells using a lentiviral vector (pGIPZ) expressing a *Map3k14*-specific shRNA as well as the green fluorescent protein (GFP), the latter of which allows enrichment of the infected cells by flow cytometric cell sorting. NIK knockdown not only attenuated the induction of IgA^+ B cells in wild-type B cells but also abrogated the hyper-induction of IgA^+ B cells in the *Tbk1*^{BKO} B cells (Fig. 5e). Similar results were obtained with a different NIK shRNA (data not shown). We also examined the effect of NIK knockdown on B cell proliferation. The *Tbk1*^{BKO} B cells displayed enhanced proliferative ability in response to anti-CD40 or BAFF stimulation as well as to LPS and anti-IgM (Supplementary Fig. 7). Interestingly, the hyper-proliferative phenotype of the *Tbk1*^{BKO} B cells, stimulated by both the noncanonical and canonical NF-κB inducers, was dependent on NIK (Supplementary Fig. 7). One possibility is that the B cells isolated from the *Tbk1*^{BKO} mice already accumulated low amounts of NIK due to *in vivo* exposure to inducers (for example, BAFF). Collectively, these data suggest a critical role for NIK and its downstream noncanonical NF-κB in mediating the IgA hyper-production of TBK1-deficient B cells.

TBK1 is a negative regulator of NIK

Although TBK1 has been linked to antiviral innate immune response, recent work suggests the activation of this kinase by additional inducers[41, 42]. Interestingly, we found that both APRIL and BAFF stimulated potent activation of TBK1 (Fig. 6a). Since BAFF stimulates both BAFFR and TACI in B cells, we assessed the contribution of these receptors to TBK1 phosphorylation using NIH3T3 cells stably transduced with TACI or BAFFR. BAFF and APRIL stimulated prominent TBK1 activation in NIH3T3-TACI cells and weak activation of TBK1 in NIH3T3-BAFFR (Fig. 6b). This result suggests that TACI may be the predominant receptor that mediates BAFF-stimulated TBK1 activation, although the relative expression level of TACI and BAFFR may also be an influencing factor. Parallel experiments revealed that anti-CD40, as well as LPS and anti-IgM, also stimulated the phosphorylation of TBK1 (Fig. 6c).

A central signaling mechanism of the noncanonical NF-κB pathway is the fate control of NIK[15]. Under steady-state conditions, NIK undergoes basal degradation via its ubiquitination by a TRAF3-dependent ubiquitin ligase complex composed of TRAF2 and c-IAP, and induction of p100 processing involves TRAF3 degradation and NIK accumulation[15]. Interestingly, we found that the *Tbk1*deficiency promoted the induction of NIK by both anti-CD40 and BAFF (Fig. 6d). The elevated NIK protein abundance in *Tbk1*^{BKO} cells was not due to increased *Map3k14* gene expression (data not shown) and did not seem to involve upstream signaling events, since the TBK1 deficiency had no obvious effect on the degradation of TRAF3 (Fig. 6d) or the abundance of TRAF2, c-IAP2, and IKKα proteins (data not shown).

To assess whether TBK1 is directly involved in NIK regulation, we examined whether TBK1 physically interacts with NIK using wild-type B cells. Since the steady-state abundance of NIK is too low for detection, we incubated the cells with a proteasome inhibitor, MG132, to allow NIK to accumulate. In the absence of a stimulus, there was little TBK1 co-immunoprecipitated with NIK; however, upon stimulation of the cells with anti-CD40 or BAFF, TBK1 formed a stabile complex (Fig. 6e). Notably, IKKε was not recruited to NIK, despite its abundant expression in these cells (Fig. 6e). The NIK-TBK1 physical interaction was further confirmed using a transfection model, which demonstrated that TBK1, but not IKKε, interacted with NIK (Fig. 6f). These findings suggest a direct mechanism by which TBK1 controls the fate of NIK.

TBK1 induces NIK phosphorylation and degradation

To further examine the mechanism by which TBK1 regulates NIK, we tested whether TBK1 induces NIK degradation in transfected cells. Indeed, when coexpressed with TBK1, the amount of NIK, but not that of the internal control protein GFP, was severely reduced (Fig. 7a). This effect was not seen with a TBK1 kinase-dead mutant (K38A) and was blocked by a proteasome inhibitor, MG132, suggesting that TBK1 might mediate phosphorylation-dependent NIK degradation. Indeed, extended times of protein fractionation in SDS gels revealed slow-migrating forms of NIK that were induced by TBK1, probably representing phosphorylated NIK (Fig. 7b). Interestingly, the TBK1 homologue IKKε did not induce NIK degradation (Fig. 7b). Consistent with the prior finding that IKKα phosphorylates NIK[43],

IKKα and its constitutively active mutant, IKKα(SS/EE), promoted generation of the slow-migrating NIK bands (Fig. 7b). Interestingly, however, IKKα was insufficient for inducing NIK degradation (Fig. 7b). By generating a panel of NIK mutants, we found that deletion of 100 amino acids from the C-terminus of NIK generated a mutant, 1-847, that was resistant to TBK1-induced degradation, but truncation of NIK from the N-terminus up to amino acid 238 did not affect TBK1-induced NIK degradation (Fig. 7c). This result suggested that the degradation-regulatory sequence of NIK might be located in its C-terminal region. Since two of the N-terminal truncation mutants (152-947 and 238-947) lack the TRAF3-binding site[44], this finding also ruled out the involvement of TRAF3 in TBK1-stimulated NIK degradation.

To directly examine whether TBK1 mediates NIK phosphorylation, we purified mouse NIK from cells transfected with either NIK alone or NIK plus TBK1 and then performed mass spectrometry to identify the phosphorylation sites of NIK. TBK1 stimulated NIK phosphorylation at several serines (Supplementary Table 1). Most interesting was serine 862, which is conserved between human and mouse NIK and located within the degradation-determination region (amino acids 847-947) identified in the truncation studies (Fig. 7c). Mutation of this site generated a NIK point mutant, S862A, that became resistant to TBK1-induced degradation, whereas mutation of several other potential phosphorylation sites of NIK did not affect its degradation (Fig. 7d). Notably, TBK1 did not phosphorylate serines 809, 812, or 815 of NIK, which were previously shown to be phosphorylated by IKKα and to regulate the steady-state abundance of NIK[43]. Mutation of these serines also did not affect TBK1-induced NIK degradation (Fig. 7d).

To examine the role of S862 in signal-induced NIK degradation, we stably expressed wild-type NIK or the NIK S862A mutant in murine M12 B cells. The NIK S862A mutant did not show enhanced stability at steady-state (Fig. 7e). However, in response to either anti-CD40 or BAFF, the NIK S862A mutant had markedly more accumulation than the wild-type NIK (Fig. 7e). These findings further emphasize a role for TBK1-induced NIK phosphorylation in mediating NIK degradation.

To examine the functional significance of TBK1-induced NIK degradation in IgA class switching, we reconstituted the NIK-deficient B cells with NIK or NIK S862A. Reconstitution of the cells with NIK greatly promoted the induction of IgA^+ cells (Fig. 7f,g). Probably due to its constitutive activity, NIK also promoted the IgA induction in the absence of anti-CD40 or BAFF. More importantly, expression of the NIK S862A mutant resulted in even higher frequencies of IgA^+ B cells (Fig. 7f,g). Taken together, these findings suggest that TBK1-mediated NIK phosphorylation and degradation serves as a negative mechanism to prevent aberrant noncanonical NF-κB activation and IgA class switching.

DISCUSSION

The data presented in this study demonstrated a unique and unexpected role for TBK1 in controlling the production of IgA. The B cell-specific TBK1 deficiency not only causes aberrant induction of IgA by antigens but also led to the elevated steady-state concentration of serum IgA and the development of nephropathy-like symptoms in older mice. Although the induction of IgA class switching involves different signals, TBK1 specifically regulates

the costimulatory signal induced by BAFF, anti-CD40, and to a lesser extent APRIL. We obtained genetic evidence that TBK1 negatively regulates the noncanonical NF-κB pathway by controlling the fate of NIK in B cells stimulated by anti-CD40 or BAFF. Prior studies suggest that the steady-state amount of NIK is regulated by a TRAF3-dependent ubiquitin ligase composed of cIAP1 and TRAF2[15]. IKKα also mediates the phosphorylation and stability of NIK, although the *in vivo* role of this latter finding remains unclear[43]. We found that in contrast to these known regulators of NIK, TBK1 predominantly regulates the fate of NIK under inducible conditions.

Our data revealed that the TBK1 deficiency had no effect on TRAF3 degradation, suggesting that the TBK1-mediated NIK regulation does not involve upstream signaling steps. Indeed, TBK1 physically associated with NIK in a signal-dependent manner and stimulated the phosphorylation and degradation of NIK. This function of NIK appeared to be highly specific, since the TBK1 homologue IKKε did not bind NIK or induce NIK degradation. Consistently, IKKε was also dispensable for the control of IgA class switching. Recent studies suggest that TBK1 and IKKε may also inhibit the activation of the canonical IKK[42, 45]. However, TBK1 and IKKε may be functionally redundant in mediating this function, since the TBK1 deficiency in B cells only had a weak stimulatory effect on LPS-stimulated IKK activation. It is also possible that the role of TBK1 in canonical IKK regulation is cell type specific. Nevertheless, our current work demonstrates a non-redundant role for TBK1 in the regulation of NIK and noncanonical NF-κB pathway.

The noncanonical NF-κB pathway is traditionally thought to mediate the nuclear translocation of only the RelB-p52 dimer. However, theoretically, the noncanonical NF-κB pathway should regulate any NF-κB members that are sequestered by p100. In fact, it was shown almost two decades ago that a large proportion of the cytoplasmic RelA is sequestered by p100 (ref. [46]). Although RelA activation by many inducers, including TNF-α and IL-1, does not require NIK or p100 processing, the activation of RelA by noncanonical NF-κB inducers, such as anti-CD40, is partially dependent on NIK and p100 processing[16]. Thus, the function of the noncanonical NF-κB pathway is beyond what we learned from studying the RelB and *Nfκb2* KO mice. Using *Nfκb2*$^{Lym1/+}$ and NIK-deficient B cells, we showed in the present study that the noncanonical NF-κB pathway has a crucial role in regulating IgA class switching, thus explaining the impaired IgA production in *Nfκb2*$^{Lym1/+}$ and NIK mutant mice[16, 17] and the IgA hyperproduction in BAFF transgenic mice [5, 6]. Our findings also provide the molecular insight into the mechanism by which the TNF family members promote IgA class switching.

TBK1 is best known as a kinase that responds to TRIF-dependent TLRs and intracellular nucleic acid sensors [26-30]. However, recent studies suggest that TBK1 responds to previously unappreciated signals, such as those triggered by the MyD88-dependent TLRs and TNF-α[42]. Our present study further demonstrated the activation of TBK1 by signals elicited from CD40, TACI, BAFFR, as well as the BCR. Compared to TACI, BAFFR seemed to be a much weaker stimulator of TBK1. However, since BAFF stimulates both BAFFR and TACI on B cells, it is likely that the TACI-mediated TBK1 activation provides a negative signal for BAFFR-mediated induction of noncanonical NF-κB signaling. In summary, the findings of the present study provide important insight into the mechanism of

noncanonical NF-κB regulation and establish TBK1 as a pivotal regulator of this signaling pathway. Our work also demonstrates an important role for TBK1 and noncanonical NF-κB in the regulation of IgA class switching. Given the involvement of the noncanonical NF-κB pathway in various biological processes, these findings have implications for the development of new therapeutic approaches.

METHODS

Mice

Tbk1-floxed mice were generated using the LoxP targeting system (Taconic). The *Tbk1*-floxed mice were crossed with CD19-Cre transgenic mice (Jackson Lab) to produce age-matched $Tbk1^{+/+}Cd19^{Cre/+}$ (termed wild-type) and $Tbk1^{fl/fl}Cd19^{Cre/+}$ (termed $Tbk1^{BKO}$) mice for experiments. In some experiments, these mice were further crossed with the $Ifnar^{-/-}$ mice (kindly provided by S.S. Watowich) to generate $Tbk1^{+/+}Ifnar^{-/-}$ and $Tbk1^{BKO}Ifnar^{-/-}$ mice respectively. NIK-deficient mice[40] were provided by Amgen; IKKε-deficient mice[47] and IgM-deficient mice were from Jackson Lab; and $Nfκb2^{Lym1}$ mutant mice[16] were provided by The Water and Eliza Hall Institute of Medical Research. Since both homozygous $Nfκb2^{Lym1/Lym1}$ and heterozygous $Nfκb2^{Lym1/+}$ mice have prominent phenotype[16], the $Nfκb2^{Lym1/+}$ and age-matched wild-type controls ($Nfκb2^{+/+}$) were used in experiments. The NIK-deficient mice had a 129SvEv background, and all of the other mouse strains had a B6;129 mixed background. The mice were maintained in specific pathogen-free facility of The University of Texas MD Anderson Cancer Center, and all animal experiments were conducted in accordance with protocols approved by the Institutional Animal Care and Use Committee.

Plasmids, antibodies, and reagents

The pcDNA expression vectors encoding HA-tagged human NIK and its truncation mutants (NIK1-847, NIK1-810, NIK1-745, NIK33-947, NIK152-947 and NIK238-947) were as described[48]. pCLXSN(GFP)-murine (m) NIK was generated by inserting murine NIK cDNA into a modified GFP-expressing pCLXSN vector, pCLXSN(GFP)[49], and the pCLXSN(GFP)-based mouse NIK S862A, NIK S862D, and NIK S862E mutants were created by site-directed mutagenesis using a QuickChange II Site-Directed Mutagenesis Kit (Stratagene). FLAG-tagged mNIK and mNIK S809/812/815A (in pcDNA vector) were provided by G. Cheng[43], and FLAG-tagged mNIK S820/821A, mNIK S862A, mNIK S883/886/887A, and mNIK S895/898A were created by site-directed mutagenesis. FLAG-tagged TBK1 and its catalytically inactive mutant (TBK1 K38A) were provided from C. Wang, HA-IKKα and HA-IKKαSSEE were provided by M. Karin, and FLAG-IKKε (IKKi) was provided by S. Akira.

Goat anti-mouse IgM F(ab')2 (anti-IgM) and anti-mouse CD40 (553788) (used for B cell stimulation) were from Jackson ImmunoResearch Laboratories and BD Bioscience, respectively. Antibodies for TBK1 (108A429), c-Rel (sc-71), IRF3 (FL0425), c-IAP2 (H-85), IKKα (H744), RelB (C-19), Lamin B (C-20), IKKε (IKKi, H-116), IKKγ (FL419), NIK (H248), TRAF2 (C-20), and TRAF3 (C-20) were from Santa Cruz Biotechnology. Antibodies for Actin (C-4) and p52 (SP1494) were from Sigma and NCI Preclinical

Repository, respectively. Phospho-TBK1 (pTBK1, Ser172) (D52C2) was from Cell Signaling Technology, and phospho-IRF3 was from Pierce. HRP-conjugated anti-HA (HA-7) and HRP-conjugated anti-FLAG (M2) were from Sigma-Aldrich. Fluorescence-labeled antibody reagents are listed in the section of flow cytometry and cell sorting.

The recombinant hTGF-β and BAFF were from PeproTech. LPS (derived from *Escherichia coli* strain 0127:B8) and APRIL (*Mega*APRIL) were from Sigma-Aldrich and Enzo Life Sciences, respectively.

Cell lines

The murine B cell line M12.4.1 (called M12 in this paper) and human embryonic kidney (HEK) 293 cell lines were described previously[44]. NIH3T3 cells stably infected with the MigR1 retroviral vector, MigR1-BAFFR, or MigR1-TACI were provided by M.P. Cancro[24].

Mouse immunization, antibody detection, and renal-function analyses

Age-matched wild-type and *Tbk1*^{BKO} mcie (6-8 weeks old) mice were injected intraperitoneally (i.p.) with 0.2 ml of NP-KLH, NP-Ficoll, or NP-LPS (0.1 mg/ml in PBS). Sera were collected at the indicated times after immunization and subjected to ELISAs (Southern Biotechnology Associates).

Serum and urine were collected from unimmunized mice (8 months old). Autoantibodies for dsDNA and nuclear antigen were measured by using specific ELISA kits (Alpha Diagnostic Intl, Inc.). Renal function was determined by measuring the concentrations of urinary protein (Rat Urinary Protein Assay Kit, Chondrex, lnc.), blood urea nitrogen (Urea Nitrogen Reagent Set, Bio-Quant, Inc.) and serum creatinine (Creatinine Assay Kit, Cayman Chemical Company).

Flow cytometry and cell sorting

Single-cell suspensions of bone marrow, spleen, or lymph nodes were subjected to flow cytometry and cell sorting using FACSAria (BD Bioscience)[50]. The fluorescence-labeled antibodies that were used included FITC-conjugated anti-IgA (BD Bioscience, C10-3), anti-IgG1 (BD Bioscience, A85-1), anti-CD21 (BD Bioscience, 7G6); Alexa Fluor 488-conjugated anti-IgG (H+L) (Invitrogen, A11001); PE-conjugated anti-IgA (BD Bioscience, 11-44-2), anti-B220 (BD Bioscience, RA3-6B2), anti-CD23 (BD Bioscience, B3B4); PE-Cy7-conjugated anti-CD19 (eBioscience, 1D3); PerCP5.5-conjugated anti-IgM (eBioscience, R6-60.2); and APC-conjugated anti-IgD (eBioscience, 11-26).

B-cell purification and IgA class-switching assays

B cells were purified from splenocytes using anti-B220-conjugated magnetic beads (Miltenyl Biotec) and cultured in 3 replicate wells of 24-well plates (5×10^5 cells/well). The purified B cells were cultured for 5 days in medium in the presence of LPS (1 μag/ml), recombinant human APRIL (200 ng/ml), human TGF-β (2 ng/ml), anti-mCD40 (1 μg/ml), or BAFF (200 ng/ml). The frequency of B cells expressing IgA isotype was measured by flow cytometry using FITC-conjugated anti-mouse IgA. For examining IgG1 and IgA class switching, TGF-β and APRIL were replaced by IL-4 (40 ng/ml) in the reaction. Germ-line

transcript (GLT) for IgA (αGLT) and IgG1 (γ1GLT) were quantified by real-time quantitative PCR (qPCR). For *in vivo* induction of the IgA class switching, mice were immunized i.p. with 0.2 ml of sheep red blood cells (SRBC) (1×10^9/ml in PBS). After 5 days, splenocytes and lymph node cells were subjected to flow cytometry to detect IgA^+ B cells.

B cell proliferation assay

Purified B cells were stimulated with anti-IgM (10 μg/ml), LPS (100 ng/ml), poly IC (20 μg/ml), anti-CD40 (1 μg/ml) or BAFF (200 ng/ml) in replicate wells of 96-well plates (1×10^5 cells per well) at 37 °C. After stimulation for 40 h, B cells were pulse-labeled for 6 h with [^{3}H]thymidine and then harvested for thymidine-incorporation assays.

B cell adoptive transfer

Mature $CD19^+IgM^+$ B cells were purified from the spleen of wild-type (GFP^+) and *Tbk1*^{BKO} (GFP^-) mice by flow cytometry. The wild-type and *Tbk1*^{BKO} B cells were transferred (i.v.), either separately or as a mixture (1:1 ratio), into the B cell-deficient *IgM*$^{-/-}$ mice (1×10^7 cells/recipient mouse). After 6 h, these mice were immunized (i.p.) with 1 ml of SRBC and sacrificed after 7 days for quantifying the IgA^+ B cells by flow cytometry.

NIK knockdown and overexpression in primary B cells

To produce the lentiviral particles, the pGIPZ vectors, either empty (pGIPZ) or encoding NIK shRNA (pGIPZ-shNIK), were transfected into HEK293 cells (using calcium method) along with the packaging vectors psPAX2 and pMD2 (provided by X. Qin). Primary B cells were stimulated for 8 hrs with LPS (5 μg/ml) and then infected with lentiviruses carrying either pGIPZ or pGIPZ-shNIK. After 72 h, the infected cells were enriched by flow cytometric cell sorting (based on GFP expression) and subsequently used for *in vitro* IgA class-switching experiments. NIK was also knocked down using a different NIK shRNA encoded by the pLKO.1 lentiviral vector. 24 h after the infection, the cells were selected with puromycin along with *in vitro* IgA class-switching assays. The target sequence of the two NIK shRNAs are: pGIPZ-shNIK: 5′-AGTCTGAGAGTCTCGATCA-3′ pLKO.1-shNIK: 5′-CAGGAAGATGAGTCTCCACTA-3′

For NIK expression, retroviruses were produced by transfecting the HEK293 cells with an empty pCLXSN(GFP) vector or the same vector encoding NIK or its point mutants along with the VSV-G and pCL-Ampho packaging vectors. The virus-containing supernatants were used for infecting the LPS-stimulated splenic B cells, and the infected cells were subjected to IgA class-switching assays.

NIK purification and mass spectrometry

HEK 293T cells were co-transfected with plasmids encoding HA-NIK and FLAG-TBK1; 48 h after transfection, cells were treated with MG132 for additional 2 h. NIK protein was immunoprecipitated as described above with Anti-HA affinity agarose (Roche) and proteins were eluted with protein solubilization buffer. Mass spectrometry was performed and analyzed by Mass Spectrometry Facility at Harvard University.

Ubiquitination assay

293 T cells were transfected with HA-NIK with FLAG-TBK1 or FLAG-TBK1 K38A. Total cell lysates were collected 48 h after transfection. Cells were lysed in radioimmunoprecipitation assay (RIPA) buffer supplemented with 1 mM N-ethylmaleimide. Lysates were immediately heated for 5 min in the presence of 1% (wt/vol) SDS and then were diluted ten times with RIPA buffer. Ubiquitinated NIK was isolated by immunoprecipitation (IP) and was detected by immunoblot analysis with the anti-ubiquitin (Santa Cruz, P4D1).

Immunofluorescence

Kidneys from 8-month old mice were rapidly frozen in Tissue-Tec OCT compound (VWR International) using liquid nitrogen-prechilled 2-methlbutane. The frozen tissues were stored at −70 °C until processed to produce 2 μm cryostat sections. The sections were fixed in 100% acetone for 15 min and stained with either fluorescein isothiocyanate (FITC)-labeled rat anti-mouse IgA or phycoerythrin (PE)-labeled rat anti-mouse IgM (BD Bioscience) at 2 μg/ml overnight at 4 °C.

Real-time quantitative RT-PCR (QPCR)

Total RNA was isolated using TRI reagent (Molecular Research Center, Inc.) and subjected to cDNA synthesis using RNase H-reverse transcriptase (Invitrogen) and oligo (dT) primers. Real-time quantitative PCR was performed in triplicates, using iCycler Sequence Detection System (Bio-Rad) and iQTM SYBR Green Supermix (Bio-Rad). The expression of individual genes was calculated by a standard curve method and normalized to the expression of *Actb*. The gene-specific primer sets used (all for mouse genes) were *Map3k14*, 5′-TGCGACTTTGGCCACGCCTT-3′ and 5′-GCCATGTGGGTCTCCGTGCC-3′; *Actb*, 5′-CGTGAAAAGATGACCCAGATCA-3′ and 5′-CACAGCCTGGATGGCTACGT-3′; αGLT, 5′-CAAGAAGGAGAAGGTGATTCAG-3′ and 5′-GAGCTGGTGGGAGTGTCAGTG-3′; γ1GLT, 5′-GGCCCTTCCAGATCTTTGAG-3′and 5′-ATGGAGTTAGTTTGGGCAGCA-3′; *Aicda*, 5′-GCCACCTTCGCAACAAGTCT-3′and 5′-CCGGGCACAGTCATAGCAC-3′.

Immunoblot analysis, EMSA, and kinase assays

Purified B cells were stimulated with anti-IgM (10 μg/ml), LPS (1 μg/ml), APRIL (200 ng/ml), anti-CD40 (1 μg/ml) or BAFF (500 ng/ml) for the indicated times. Total and subcellular extracts were prepared from the cells and subjected to immunoblotting (IB) and electrophoretic mobility shift assays (EMSA). In some experiments, the protein bands were quantified using the ImmageJ software. In the case of protein-phosphorylation analyses and kinase assays, cells were lysed in a kinase cell lysis buffer supplemented with phosphatase inhibitors. IKK was isolated by IP using IKKγ and subjected to kinase assays using a GST fusion protein containing the N-terminal 54 amino acids of IκBα (GST-IκBα(1-54)) as substrate [51].

Statistical analysis

Prism software was used for two-tailed unpaired *t*-tests. *P*-values < 0.05 or 0.01 were considered significant and very significant, respectively.

Supplementary Material

Refer to Web version on PubMed Central for supplementary material.

ACKNOWLEDGEMENTS

We would like to thank Amgen, Water Eliza Hall Institute of Medical Research, and S.S. Watowich for *Map3k14* KO, *Nfκb2*^{Lym1}, and *Ifnra*$^{-/-}$ mice, respectively; S. Akira (Osaka University), G. Cheng (University of California, Los Ageles), M. Karin (University of California, San Diego), X. Qin (Sun Yat-Sen University), and Chen Wang (Shanghai Institutes for Biological Sciences) for plasmid vectors; and M. P Cancro (University of Pennsylvania) for NIH3T3 cell lines. We also thank the personnel from the animal facility, flow cytometry, DNA analysis, and histology core facilities at MD Anderson Cancer Center for their technical assistance. This study was supported by grants from National Institutes of Health (AI057555, AI064639, GM84459, and T32CA009598).

REFERENCES

1. Macpherson AJ, McCoy KD, Johansen FE, Brandtzaeg P. The immune geography of IgA induction and function. Mucosal Immunol. 2008; 1:11–22. [PubMed: 19079156]
2. Park MA, Li JT, Hagan JB, Maddox DE, Abraham RS. Common variable immunodeficiency: a new look at an old disease. Lancet. 2008; 372:489–502. [PubMed: 18692715]
3. Papista C, Berthelot L, Monteiro RC. Dysfunctions of the Iga system: a common link between intestinal and renal diseases. Cell. Mol. Immunol. 2011; 8:126–134. [PubMed: 21278767]
4. Wang J, et al. Dysregulated LIGHT expression on T cells mediates intestinal inflammation and contributes to IgA nephropathy. J. Clin. Invest. 2004; 113:826–835. [PubMed: 15067315]
5. McCarthy DD, Chiu S, Gao Y, Summers-deLuca LE, Gommerman JL. BAFF induces a hyper-IgA syndrome in the intestinal lamina propria concomitant with IgA deposition in the kidney independent of LIGHT. Cell. Immunol. 2006; 241:85–94. [PubMed: 16987502]
6. McCarthy DD, et al. Mice overexpressing BAFF develop a commensal floradependent, IgA-associated nephropathy. J. Clin. Invest. 2011; 121:3991–4002. [PubMed: 21881212]
7. Cazac BB, Roes J. TGF-beta receptor controls B cell responsiveness and induction of IgA in vivo. Immunity. 2000; 13:443–451. [PubMed: 11070163]
8. Litinskiy MB, et al. DCs induce CD40-independent immunoglobulin class switching through BLyS and APRIL. Nat. Immunol. 2002; 3:822–829. [PubMed: 12154359]
9. Castigli E, et al. TACI and BAFF-R mediate isotype switching in B cells. J. Exp. Med. 2005; 201:35–39. [PubMed: 15630136]
10. Castigli E, et al. Impaired IgA class switching in APRIL-deficient mice. Proc. Natl. Acad. Sci. USA. 2004; 101:3903–3908. [PubMed: 14988498]
11. Cerutti A. The regulation of IgA class switching. Nat. Rev. Immunol. 2008; 8:421–434. [PubMed: 18483500]
12. Tezuka H, et al. Prominent role for plasmacytoid dendritic cells in mucosal T cellindependent IgA induction. Immunity. 2011; 34:247–257. [PubMed: 21333555]
13. Hayden MS, Ghosh S. Shared principles in NF-kappaB signaling. Cell. 2008; 132:344–362. [PubMed: 18267068]
14. Vallabhapurapu S, Karin M. Regulation and function of NF-kappaB transcription factors in the immune system. Annu. Rev. Immunol. 2009; 27:693–733. [PubMed: 19302050]
15. Sun SC. The noncanonical NF-kappaB pathway. Immunol. Rev. 2012; 246:125–140. [PubMed: 22435551]
16. Tucker E, et al. A novel mutation in the Nfkb2 gene generates an NF-kappa B2 "super repressor". J. Immunol. 2007; 179:7514–7522. [PubMed: 18025196]

17. Shinkura R, et al. Alymphoplasia is caused by a point mutation in the mouse gene encoding Nf-kappa b-inducing kinase. Nat. Genet. 1999; 22:74–77. [PubMed: 10319865]
18. Caamano JH, et al. Nuclear factor (NF)-kappa B2 (p100/p52) is required for normal splenic microarchitecture and B cell-mediated immune responses. J. Exp. Med. 1998; 187:185–196. [PubMed: 9432976]
19. Franzoso G, et al. Mice deficient in nuclear factor (NF)-kappa B/p52 present with defects in humoral responses, germinal center reactions, and splenic microarchitecture. J. Exp. Med. 1998; 187:147–159. [PubMed: 9432973]
20. Snapper CM, et al. B cells lacking RelB are defective in proliferative responses, but undergo normal B cell maturation to Ig secretion and Ig class switching. J. Exp. Med. 1996; 184:1537–1541. [PubMed: 8879226]
21. Mackay F, Schneider P. TACI, an enigmatic BAFF/APRIL receptor, with new unappreciated biochemical and biological properties. Cytokine Growth Factor Rev. 2008; 19:263–276. [PubMed: 18514565]
22. Hauer J, et al. TNF receptor (TNFR)-associated factor (TRAF) 3 serves as an inhibitor of TRAF2/5-mediated activation of the noncanonical NF-kappaB pathway by TRAF-binding TNFRs. Proc Natl Acad Sci U S A. 2005; 102:2874–2879. [PubMed: 15708970]
23. Chang SK, Arendt BK, Darce JR, Wu X, Jelinek DF. A role for BLyS in the activation of innate immune cells. Blood. 2006; 108:2687–2694. [PubMed: 16825497]
24. Stadanlick JE, et al. Tonic B cell antigen receptor signals supply an NF-kappaB substrate for prosurvival BLyS signaling. Nat. Immunol. 2008; 9:1379–1387. [PubMed: 18978795]
25. Suzuki K, Meek B, Doi Y, Honjo T, Fagarasan S. Two distinctive pathways for recruitment of naive and primed IgM+ B cells to the gut lamina propria. Proc. Natl. Acad. Sci. USA. 2005; 102:2482–2486. [PubMed: 15695334]
26. Fitzgerald KA, et al. IKKepsilon and TBK1 are essential components of the IRF3 signaling pathway. Nat. Immunol. 2003; 4:491–496. [PubMed: 12692549]
27. Sharma S, et al. Triggering the interferon antiviral response through an IKK-related pathway. Science. 2003; 300:1148–1151. [PubMed: 12702806]
28. McWhirter SM, et al. IFN-regulatory factor 3-dependent gene expression is defective in Tbk1-deficient mouse embryonic fibroblasts. Proc. Natl. Acad. Sci. USA. 2004; 101:233–238. [PubMed: 14679297]
29. Hemmi H, et al. The roles of two IkappaB kinase-related kinases in lipopolysaccharide and double stranded RNA signaling and viral infection. J. Exp. Med. 2004; 199:1641–1650. [PubMed: 15210742]
30. Perry AK, Chow EK, Goodnough JB, Yeh WC, Cheng G. Differential requirement for TANK-binding kinase-1 in type I interferon responses to toll-like receptor activation and viral infection. J. Exp. Med. 2004; 199:1651–1658. [PubMed: 15210743]
31. Bonnard M, et al. Deficiency of T2K leads to apoptotic liver degeneration and impaired NF-κB-dependent gene transcription. EMBO J. 2000; 19:4976–4985. [PubMed: 10990461]
32. Tomino Y. IgA nephropathy: lessons from an animal model, the ddY mouse. J. Nephrol. 2008; 21:463–467. [PubMed: 18651534]
33. Kim RJ, et al. IL-4-induced AID expression and its relevance to IgA class switch recombination. Biochem. Biophys. Res. Commun. 2007; 361:398–403. [PubMed: 17645870]
34. Lorenz M, Jung S, Radbruch A. Switch transcripts in immunoglobulin class switching. Science. 1995; 267:1825–1828. [PubMed: 7892607]
35. Muramatsu M, et al. Class switch recombination and hypermutation require activation-induced cytidine deaminase (AID), a potential RNA editing enzyme. Cell. 2000; 102:553–563. [PubMed: 11007474]
36. Hiscott J. Triggering the innate antiviral response through IRF-3 activation. J. Biol. Chem. 2007; 282:15325–15329. [PubMed: 17395583]
37. Clément JF, Meloche S, Servant MJ. The IKK-related kinases: from innate immunity to oncogenesis. Cell Res. 2008; 18:889–899. [PubMed: 19160540]
38. Sakurai D, et al. TACI regulates IgA production by APRIL in collaboration with HSPG. Blood. 2007; 109:2961–2967. [PubMed: 17119122]

39. Bossen C, et al. Interactions of tumor necrosis factor (TNF) and TNF receptor family members in the mouse and human. J. Biol. Chem. 2006; 281:13964–13971. [PubMed: 16547002]
40. Yin L, et al. Defective lymphotoxin-beta receptor-induced NF-kappaB transcriptional activity in NIK-deficient mice. Science. 2001; 291:2162–2165. [PubMed: 11251123]
41. Kawai T, Akira S. The role of pattern-recognition receptors in innate immunity: update on Toll-like receptors. Nat. Immunol. 2010; 11:373–384. [PubMed: 20404851]
42. Clark K, Takeuchi O, Akira S, Cohen P. The TRAF-associated protein TANK facilitates cross-talk within the I{kappa}B kinase family during Toll-like receptor signaling. Proc. Natl. Acad. Sci. USA. 2011; 108:17093–17098. [PubMed: 21949249]
43. Razani B, et al. Negative feedback in non-canonical NF-κB signaling modulates NIK stability through IKKα-mediated phosphorylation. Sci. Sig. 2010; 3(123):ra41.
44. Liao G, Zhang M, Harhaj EW, Sun SC. Regulation of the NF-kappaB-inducing kinase by tumor necrosis factor receptor-associated factor 3-induced degradation. J Biol Chem. 2004; 279:26243–26250. [PubMed: 15084608]
45. Clark K, et al. Novel cross-talk within the IKK family controls innate immunity. Biochem. J. 2011; 434:93–104. [PubMed: 21138416]
46. Sun S-C, Ganchi PA, Beraud C, Ballard DW, Greene WC. Autoregulation of the NF-κB transactivator Rel A (p65) by multiple cytoplasmic inhibitors containing ankyrin motifs. Proc. Natl. Acad. Sci. USA. 1994; 91:1346–1350. [PubMed: 8108414]
47. Tenoever BR, et al. Multiple functions of the IKK-related kinase IKKepsilon in interferon-mediated antiviral immunity. Science. 2007; 315:1274–1278. [PubMed: 17332413]
48. Xiao G, Sun SC. Negative regulation of the nuclear factor kappa B-inducing kinase by a cis-acting domain. J. Biol. Chem. 2000; 275:21081–21085. [PubMed: 10887201]
49. Reiley W, Zhang M, Wu X, Graner E, Sun S-C. Regulation of the deubiquitinating enzyme CYLD by IkappaB kinase gamma-dependent phosphorylation. Mol. Cell. Biol. 2005; 25:3886–3895. [PubMed: 15870263]
50. Reiley WW, et al. Regulation of T cell development by the deubiquitinating enzyme CYLD. Nat. Immunol. 2006; 7:411–417. [PubMed: 16501569]
51. Uhlik M, et al. NF-kappaB-inducing kinase and IkappaB kinase participate in human T-cell leukemia virus I Tax-mediated NF-kappaB activation. J. Biol. Chem. 1998; 273:21132–21136. [PubMed: 9694868]

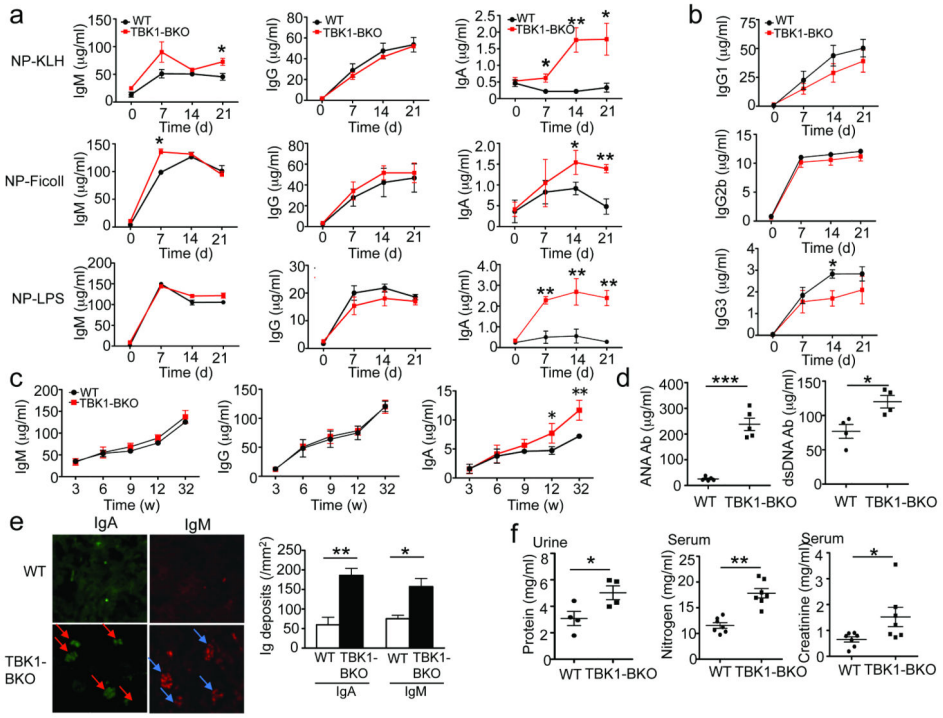

Figure 1. B cell ablation of TBK1 causes hyperproduction of IgA and autoantibodies, coupled with nephropathy-like symptoms

(**a,b**) ELISA of NP-specific antibody isotypes in the sera of wild-type (WT) and *Tbk1*^{BKO} mice (6-week old) immunized i.p. with NP-KLH, NP-Ficoll or NP-LPS (**a**) or with NP-KLH (**b**). Data are presented as mean ± S.D. of six animals and representative of three independent experiments. (**c, d**) ELISA of the basal concentrations of Ig isotypes (**c**) or antinuclear antigen (ANA) and anti-double-stranded DNA (dsDNA) auto-antibodies (**d**) in the sera of different ages of unimmunized WT and *Tbk1*^{BKO} mice (32 weeks in **d**). Data are presented as mean ± S.D. of 4-6 animals and representative of three independent experiments. (**e**) Immunofluorescence analyses of IgA and IgM deposition using kidney sections from 8-month-old WT and *Tbk1*^{BKO} mice. Data are presented as a representative picture (left, arrows indicate Ig-deposited glomeruli) and summary graph (right), representative of three independent experiments. (**f**) Concentrations of urinary protein and serum nitrogen and creatinine were measured in 8-month old WT and *Tbk1*^{BKO} mice. Data are presented as mean±S.D. of multiple mice (each symbol represents an individual mouse) and representative of 3 independent experiment. *P<0.05 and **P<0.01.

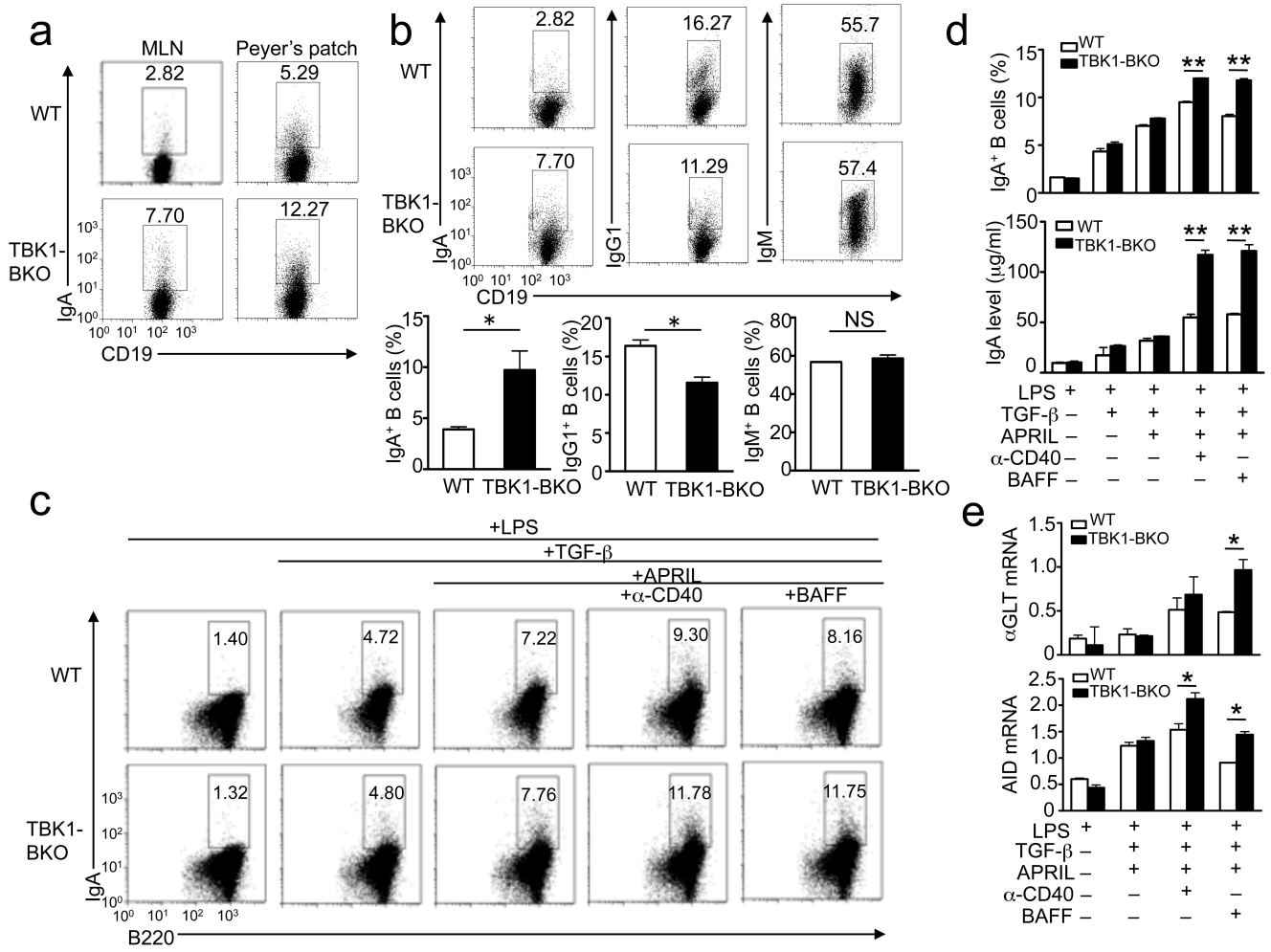

Figure 2. TBK1 negatively regulates IgA class switching induced by TNF family members

(**a**) Flow cytometry analyses of the frequency of IgA$^+$ B cells within the mesenteric lymph nodes (MLN) and Peyer's patches of non-immunized WT and *Tbk1*^{BKO} mice (8 months of age). Data are representative of three independent experiments. (**b**) Flow cytometry analysis of the frequency of IgA$^+$, IgG1$^+$, and IgM$^+$ B cells (within the splenic B cells) of WT and *Tbk1*^{BKO} mice (6 weeks of age) immunized with SRBC for day 7. Data are presented as a representative plot (upper) and summary graphs (lower) and are representative of three independent experiments. (**c, d**) Splenic B cells were cultured in the presence of LPS (1 μg/ml), either alone or in combination with other indicated inducers: TGF-β (2 ng/m l), APRIL (200 ng/ml), anti-CD40 (1 μg/ml), or BAFF (200 ng/ml). On day 5, intracellular IgA was quantified by flow cytometry (numbers indicate percentage of IgA$^+$ B cells). Data are representative (**c**) or summary (**d**, upper panel) of three independent experiments. The concentration of secreted IgA in the culture supernatants was measured by ELISA (**d**, lower). Data are presented as mean±SD of three independent experiments. (**e**) Splenic B cells were cultured as in **c** and collected on day 4 for α*GLT* and *Aicda* QPCR analysis. Actin beta *(Actb)* was used as an internal control. Data are representative of three independent experiments. *P<0.05 and **P<0.01.

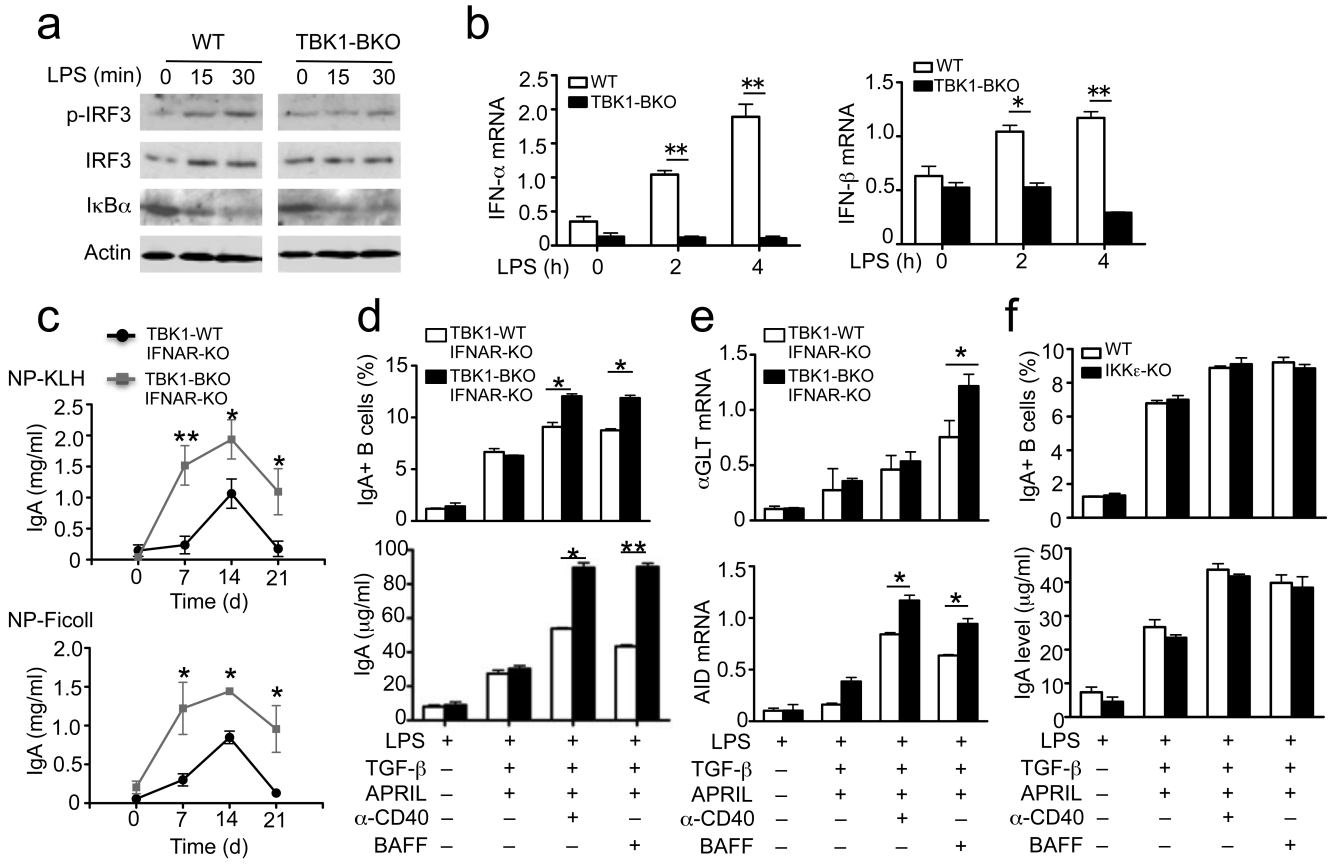

Figure 3. IgA class switching is not affected by the genetic deficiencies of *Ifnar1* or *IKKε*

(a,b) Spleen B cells of WT and *Tbk1*^{BKO} mice were stimulated with LPS (5 μg/ml) and subjected to immunoblotting (**a**) and real-time QPCR (**b**) assays. Data are representative of three independent experiments. (**c**) ELISA of NP-specific IgA in the sera of the indicated mice (6 weeks of age) immunized with NP-KLH or NP-Ficoll for the indicated times. Data are presented as mean±S.D. of three animals and representative of three independent experiments. (**d-f**) Splenic B cells from the indicated mice were cultured in the presence (+) or absence (−) of the indicated inducers as described in Fig. 2c. On day 5, the frequency of IgA^{+} B cells (upper) and the concentration of secreted IgA in the culture supernatant (lower) were quantified by flow cytometry and ELISA, respectively (**d**). The day 4 culture was collected for α*GLT* and *Aicda* QPCR analyses (**e,f**). *P<0.05 and **P<0.01. Data are representative of three independent experiments.

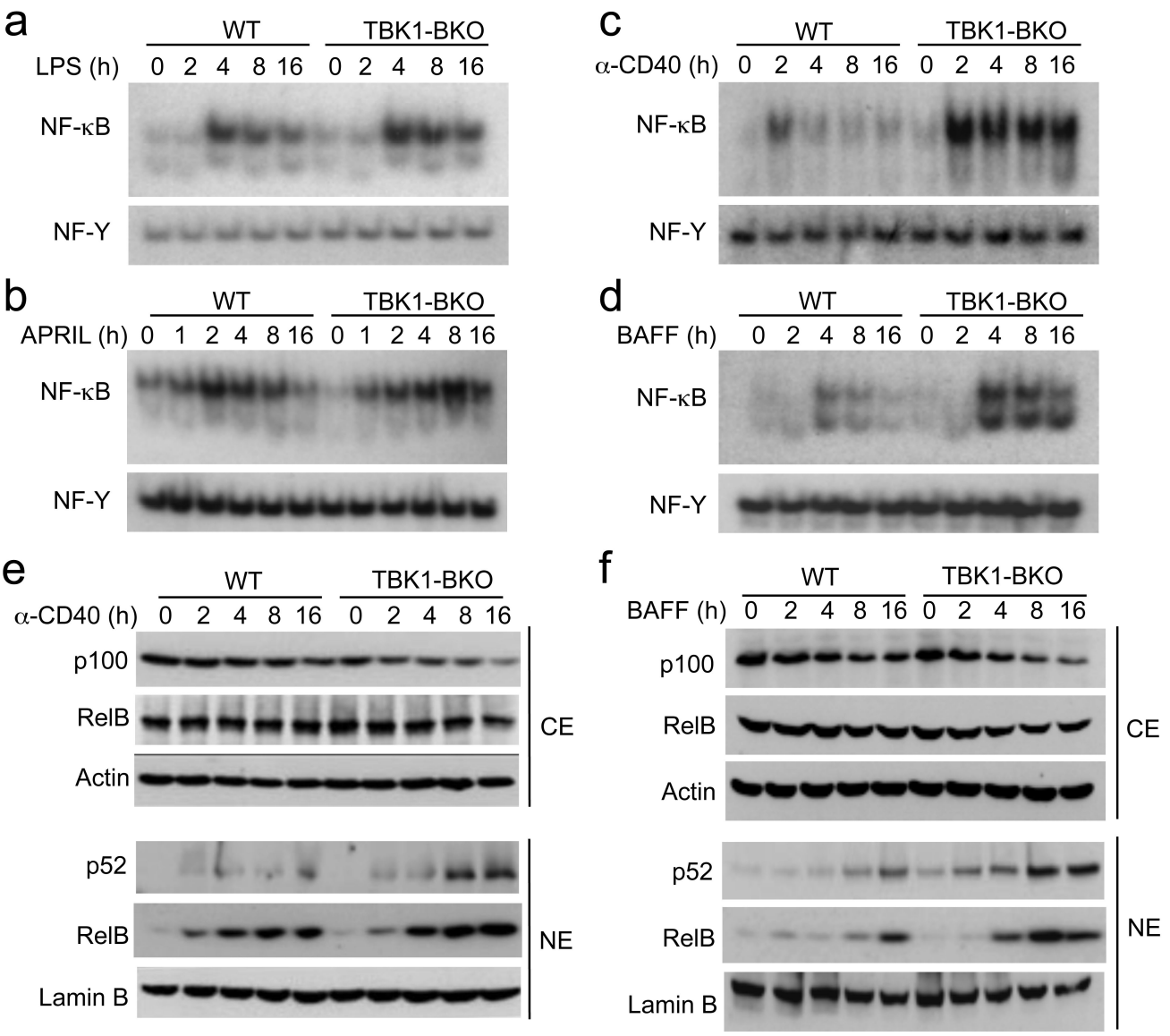

Figure 4. TBK1 is a pivotal negative regulator of the noncanonical NF-κB pathway

(**a-d**) B cells were purified from the spleen of WT or *Tbk1*^{BKO} mice (6 weeks old) and stimulated for the indicated times with LPS (1 μg/ml), APRIL (200 ng/ml), anti-CD40 (1 μg/ml), or BAFF (500 ng/ml). Nuclear extracts were subjected to EMSA using ^{32}P-radiolabeled probes bound by NF-κB or the control nuclear factor-Y (NF-Y). (**e, f**) Immunoblot analyses of the indicated NF-κB proteins or the loading control proteins (Actin and LaminB) in the cytoplasmic (CE) or nuclear (NE) extracts of the stimulated B cells. Data are representative of three independent experiments.

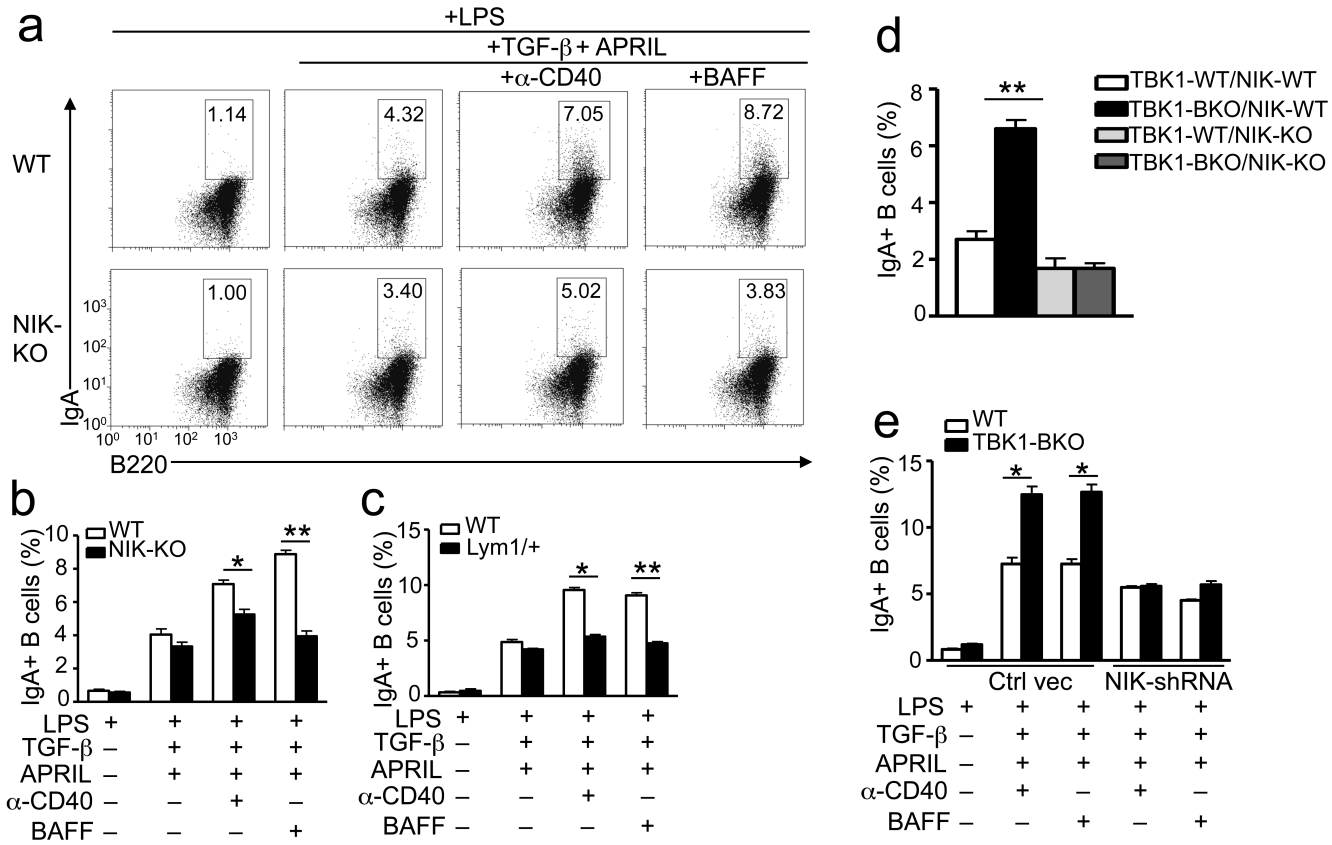

Figure 5. The noncanonical NF-κB pathway is required for IgA class switching

(**a-c**) Splenic B cells were isolated from *Map3k14* KO and WT littermate control mice (**a,b**) or *nfκb2*$^{Lym1/+}$ and *nfκb2*$^{+/+}$ (WT) littermate control mice (**c**) and cultured in the presence (+) or absence (−) of the indicated inducers. On day 5, the percentage of IgA^{+} B cells was quantified by flow cytometry. Data are representative (**a**) or summary (**b,c**) of three independent experiments. (**d**) Flow cytometry analyses of the frequency of IgA^{+} B cells within the splenic CD19^{+} B cells of indicated mice (6 week old) immunized with SRBC for 7 days. (**e**) Purified WT or *Tbk1*^{BKO} B cells were stimulated with LPS (5 μg/ml) for 8 hrs and then infected with the GFP-expressing pGIPZ vector (vector) or the same vector expressing a NIK-specific shRNA (NIK shRNA). 24 hrs after infection, B cells were cultured in the presence (+) or absence (−) of the indicated inducers and subjected to *in vitro* IgA class-switching assays. The frequency of IgA^{+} cells within the infected B-cell population was quantified by flow cytometry (gated on GFP^{+} cells). Data are mean±S.D. of two independent experiments. *P<0.05 and **P<0.01.

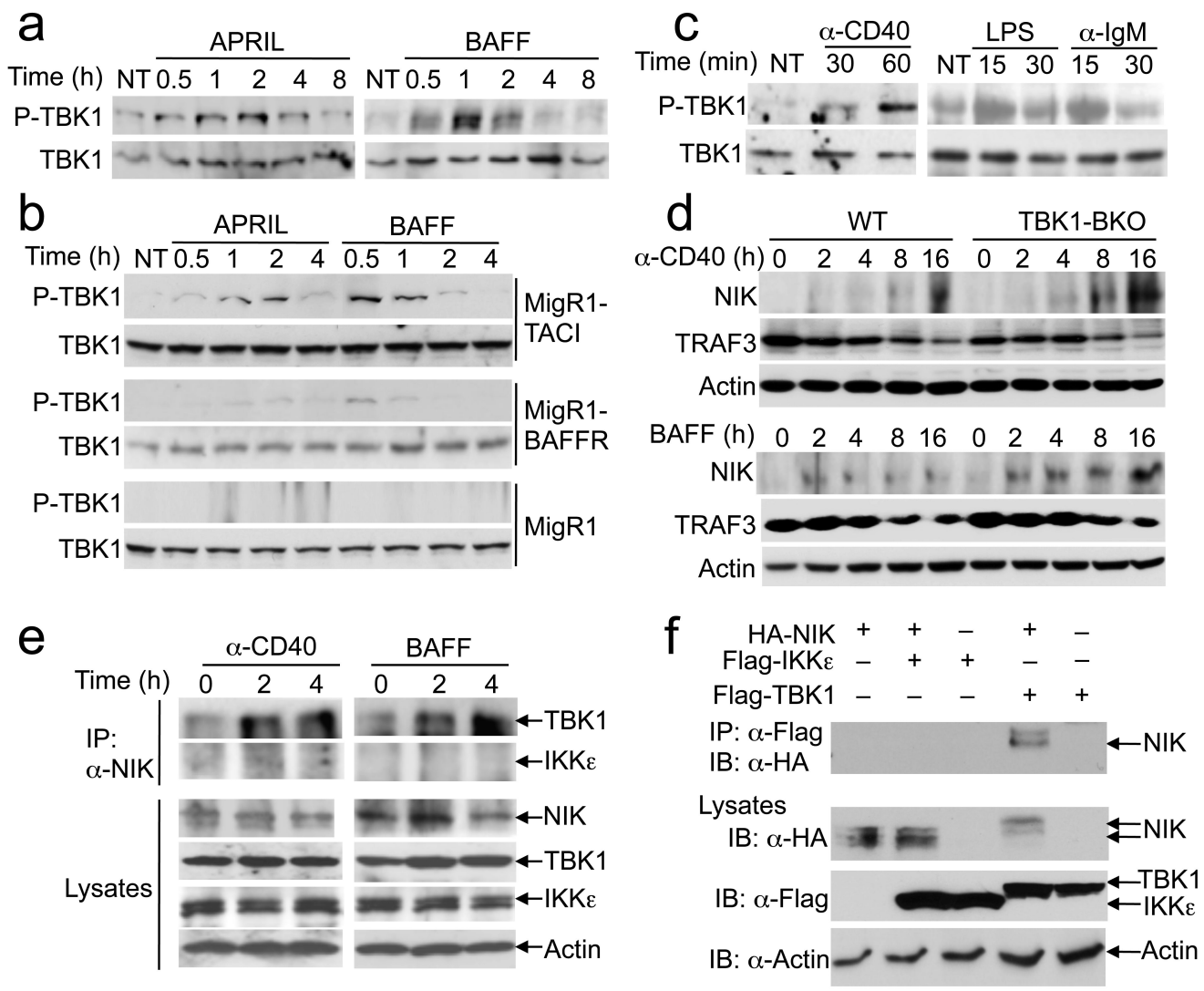

Figure 6. TBK1 is activated by the TNF family of IgA inducers and negatively regulates NIK induction

(**a**) Purified WT B cells were either not treated (NT) or stimulated with APRIL (200 ng/ml) or BAFF (500 ng/ml) for the indicated time periods and subjected to immunoblot analyses of phosphorylated (P-TBK1) and total TBK1. Data are representative of two independent experiments. (**b**) Immunoblot analyses of P-TBK1 and TBK1 in NIH3T3 cells stably infected with the empty MigR1 retroviral vector, MigR1-BAFFR, or MigR1-TACI, which were either not treated (NT) or stimulated as indicated. Data are representative of two independent experiments. (**c**) Immunoblot analyses of P-TBK1 and TBK1 in WT spleen B cells treated as indicated. Data are representative of two independent experiments. (**d**) Immunoblot analyses of the indicated proteins in whole-cell lysates of WT and *Tbk1*^{BKO} B cells stimulated with anti-CD40 or BAFF. Data are representative of three independent experiments. (**e**) WT B cells were stimulated as indicated and further incubated for 2 hrs with a proteasome inhibitor, MG132. Whole-cell lysates were subjected to NIK IP followed by detecting NIK-associated TBK1 and IKKε by IB (top two panels). Cell lysates were also

directly subjected to IB (lower four panels). Data are representative of two independent experiments. (**f**) HEK293 cells were transfected with the indicated expression vectors. Cell lysates were subjected to IP using anti-FLAG followed by IB with anti-HA to detect the co-precipitated NIK (top panel). Cell lysates were also directly analyzed by IB (bottom three panels). Data are representative of three independent experiments.

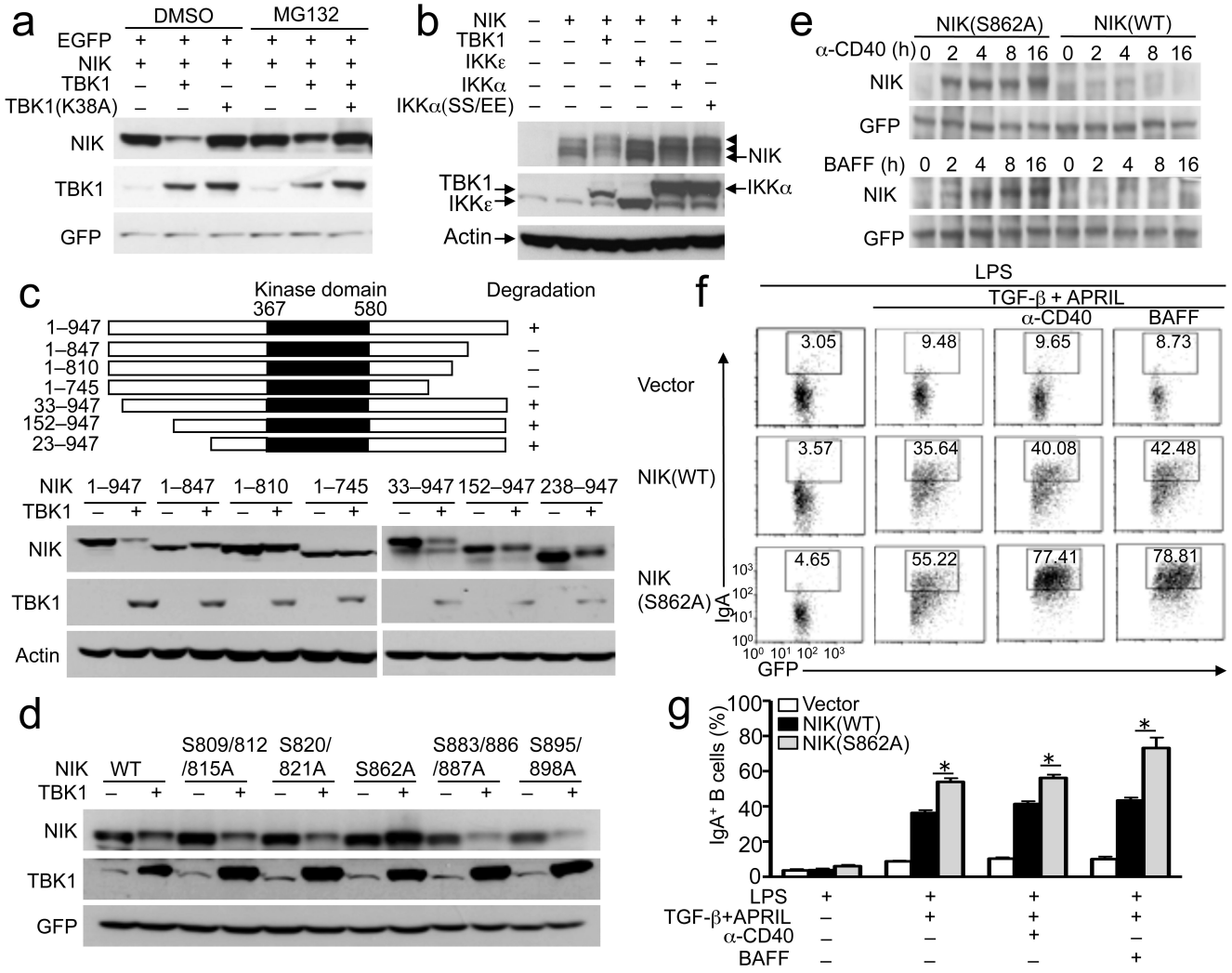

Figure 7. TBK1 induces NIK phosporylation and degradation

(**a,b**) HEK293 cells were transfected with (+) or without (−) the indicated expression vectors. After 48 hrs, the cells were incubated for 2 hours with MG132 or the solvent control DMSO (**a**) or not treated (**b**). Whole-cell lysates were subjected to IB to detect the indicated proteins. The SDS gel presented in **b** was subjected to extended time of fractionation for visualizing the more slowly migrating forms of NIK (arrowheads). Data are representative of three independent experiments. (**c, d**) IB analyses of the indicated proteins in whole-cell lysates of HEK293 cells transfected with HA-NIK or its truncation mutants (**c**) or serine point mutants (**d**) either in the presence (+) or absence (−) of FLAG-TBK1. Data are representative of three independent experiments. Diagrams of the NIK mutants are shown above panel **c**. (**e**) M12 B cells were infected with pCLXSN(GFP) retroviral vectors encoding wild-type NIK (NIK WT) or NIK S862A. Infected GFP^+ cells were sorted by flow cytometry and stimulated with anti-CD40 or BAFF. Whole-cell lysates were subjected to IB analyses of NIK and control GFP proteins. (**f,g**) Purified WT and *Tbk1*^{BKO} B cells were stimulated with LPS (5 μg/ml) for 8 hrs and then infected with empty pCLXSN(GFP)

retroviral vector (Vector) or the same vector encoding NIK WT or NIK S862A. After 24 hrs of infection, the B cells were subjected to *in vitro* IgA class switching. The frequency of IgA^+ cells within the infected B-cell population was analyzed by flow cytometry based on intracellular IgA staining and GFP expression. Data are representative (**f**) and mean±S.D. (**g**) of three independent experiments.